Chinese Journal of Chemistry, **2004**, *22*, 627—637 **Article**

Study on Osmotic Pressure and Liquid-Liquid Equilibria for Micelle, Colloid and Microemulsion Systems by Yukawa Potential

FU, Dong[a](付东) LU, Jiu-Fang*[,b](陆九芳) WU, Wei[b](吴畏) Li, Yi-Gui[b](李以圭)

[a] *Department of Environment Engineering, North China Electric Power University, Baoding, Hebei 071003, China*
[b] *Department of Chemical Engineering, Tsinghua University, Beijing 100084, China*

An equation of state (EOS) was established to study the osmotic pressure and liquid-liquid equilibria for micelle, colloid and microemulsion systems. The Carnahan-Starling equation was used for the hard sphere repulsion. The Yukawa potential was used to describe both the attractive dispersion and the double-layer repulsion. By using the established EOS, the osmotic pressures for charged colloid, uncharged micelle, uncharged and weakly charged microemuslion, the phase equilibria for uncharged micelle and charged colloid systems were studied.

Keywords osmotic pressure, liquid-liquid equilibria, micelle, colloid, microemulsion, EOS

Introduction

Dispersion systems such as micelle, colloid and microemulsion systems are of great importance in a variety of technological applications. Micelle and microemulsion systems are widely used in the fields of oil recovery, combustion, cosmetics, pharmaceuticals, agriculture, metal cutting, lubrication, food, enzymatic catalysis, organic and bio-organic reactions, polymer *etc*. Colloids such as protein and enzyme play an important role in physiological reaction of animals and humans. The separation and purification of proteins from aqueous solution become an increasingly important operation in biotechnology industry. A systematic study on micelle, colloid and microemulsion systems is meaningful either in theory or in practice. Interest in this field increased rapidly in recent years. However, properties of such systems are still not very well understood so far.

Surfactants are necessary to form the micelle and microemulsion and the critical micelle concentration (CMC) is one of the most important properties for surfactants. Below CMC, the molecules of surfactant exist in the form of monomers. However, they aggregate and form the micelles above CMC, in which there is no dispersed liquid phase.

Microemulsions are thermodynamically stable, isotropic mixtures of oil and water stabilized by surfactant and co-surfactant. They consist of nanometer sized droplets of either water-in-oil (W/O) or oil-in-water (O/W) microstructures and there is dispersed liquid phase in the core of droplets. It is usually considered that all the surfactant and co-surfactant molecules are aggregated in the interface between the dispersed liquid phase and the solvent continuum.[1]

In general, colloids are composed of solvent, dispersed particles and electrolytes. The dispersed particles immersed in the continuum are surrounded by an electric double layer, where one layer is formed by the charge in the surface of the particles and the other layer is formed by the excess of oppositely charged ions in the solution. Micelle, colloid and microemulsion systems exhibit complex phase behaviors in their phase diagrams.

Osmotic pressure, directly related to the chemical potential of solvent, is a fundamental thermodynamic property of micelle, colloid and microemulsion systems. Osmotic pressures are commonly used to determine molecular weights and characterize the interparticle interactions of such systems. The interparticle interactions and the particle sizes are the most important to the phase behaviors of such systems. Therefore, understanding the interparticle interactions is necessary in the study of osmotic pressure, as well as the description of the influence of the dispersed particle concentration on the osmotic pressure and the liquid-liquid equilibrium diagram.

Due to their great importance, many studies have been done on the interparticle interactions of dispersion systems. As we know, the cell model has been used to calculate the osmotic pressure of concentrated dispersion system.[2] Bagger-Jörgensen *et al*.[3] proposed an osmotic pressure equation for uncharged and weakly charged spherical oil-in-water microemulsion droplets.

* E-mail: jiuflu@mail.tsinghua.edu.cn
Received November 13, 2003; revised and accepted March 1, 2004.
Project supported by the National Natural Science Foundation of China (No. 20106007).

In their study, a hard-sphere repulsion combined with a van der Waals attraction is used for uncharged system, and the long-range electrostatic interaction is used for weakly charged system. They successfully described the relationship among the osmotic pressure, droplet size and interparticle interaction. Denkov *et al*.[4] proposed a theoretical model for flocculated Brownian droplets. They studied the configuration and the interaction energy of such systems and succeeded in expressing the surface bending energy in the monolayer of the surfactant and the effect of the temperatures on it. Petsev and Linse[5] developed a new equation for osmotic pressure of microemulsion and miniemulsion systems based on Denkov's work. Recently, Li *et al*.[6] studied the osmotic pressure of uncharged and weakly charged microemulsion systems by combining the Carnahan-Starling equation and cell model. Moon *et al*.[7] correlated the osmotic second virial coefficients for lysozyme from their experimental osmotic-pressure data. Wu and Prausnitz[8] used two van der Waals type models for protein solutions to high NaCl concentration range. Recently, Lin *et al*.[9] correlated and predicted the osmotic pressures for aqueous bovine serum albumin (BSA)-NaCl solutions satisfactorily based on two Yukawa potentials.

In this paper, the Carnahan-Starling equation[10] is used for the hard sphere repulsion of micelle, colloid and microemulsion systems while the Yukawa potential is used to describe both the attractive and electrostatic interactions between the dispersed particles. A new equation of state is proposed and applied to the osmotic pressure and liquid-liquid phase equilibria for some uncharged and charged dispersion systems.

Theory

Repulsion term

For systems consisting of hard spherical particles, the most accurate equation of state is given by the Carnahan-Starling equation.[10] The Helmholtz free energy A^{hs} and the compressibility factor Z^{hs} can be expressed as:

$$\frac{A^{hs}}{NkT}=\frac{4\eta-3\eta^2}{(1-\eta)^2} \tag{1}$$

$$Z^{hs}=\frac{1+\eta+\eta^2-\eta^3}{(1-\eta)^3} \tag{2}$$

η stands for the volume fraction, which can be expressed as:

$$\eta=\pi\rho\sigma^3/6 \tag{3}$$

where σ and ρ are the diameter and number density of particles, respectively.

The corresponding osmotic pressure and the chemical potential for the hard sphere contribution are expressed as:

$$\Pi^{hs}=kT\rho Z^{hs} \tag{4}$$

$$\frac{\mu^{hs}}{kT}=\ln\rho+\frac{A^{hs}}{NkT}+Z^{hs} \tag{5}$$

Attraction term

Dispersion interaction is very important for the study on phase behavior of fluids. From the perturbation theory, the Helmholtz free energy for the dispersion interaction can be expressed as:

$$A^{att}[\rho(\mathbf{r})]=\frac{1}{2}\int\int \mathrm{d}\mathbf{r}\,\mathrm{d}\mathbf{r}'\rho(\mathbf{r})\rho(\mathbf{r}')g^{ref}(\mathbf{r},\mathbf{r}')u^{att}(|\mathbf{r}-\mathbf{r}'|) \tag{6}$$

where d$\mathbf{r}$ is the infinitesimal, $\rho(\mathbf{r})$ is the number density of molecules in d$\mathbf{r}$, $g^{ref}(\mathbf{r},\mathbf{r}')$ is the radial distribution function and $u^{att}(|\mathbf{r}-\mathbf{r}'|)$ is the attractive interactions between particles. In the classical Derjaguin-Landau-Verwey-Overbeek (DLVO) theory,[11] the mean field approximation is used so that $g^{ref}(\mathbf{r},\mathbf{r}')=1$. The dispersion interaction is expressed as the Hamaker term. In this paper, the Yukawa potential is used to replace the Hamaker term because the integral equation based on Yukawa potential can be solved by the mean spherical approximation (MSA) and both the attractive interaction and the double-layer repulsion can be expressed by the same mathematic representation. Moreover, the analytic solution of Helmholtz free energy and the compressibility factor for the Yukawa potential are available from Duh and Mier-Y-Teran.[12]

The hard-core Yukawa potential is expressed as:

$$u(r)=\begin{cases}\infty & r\leqslant\sigma\\ \dfrac{-\varepsilon\exp[-\lambda(r/\sigma-1)]}{r/\sigma} & r>\sigma\end{cases} \tag{7}$$

where λ is the range parameter. Apparently, the larger the value of λ is, the steeper the potential curve is. ε is the dispersion energy parameter. According to the DLVO theory,[11] ε is defined as $\varepsilon=\varepsilon_{11}+\varepsilon_{22}-2\varepsilon_{12}$, where ε_{11}, ε_{22} and ε_{12} stand for the dispersion energy between solvent molecules, particles and between solvent molecule and particle, respectively.

The Helmholtz free energy A^{yuk} and the compressibility factor Z^{yuk} can be expressed as:

$$\frac{A^{yuk}}{NkT}=-\frac{\alpha_0}{\phi_0}\beta\varepsilon-\frac{\lambda^3}{6\eta}\left[F(x)-F(y)-(x-y)\frac{\mathrm{d}F(y)}{\mathrm{d}y}\right] \tag{8}$$

$$Z^{\mathrm{yuk}}=-\eta\frac{\beta\varepsilon}{\phi_0}\left[\frac{\partial\alpha_0}{\partial\eta}-\frac{\alpha_0}{\phi_0}\frac{\partial\phi_0}{\partial\eta}\right]+\frac{\lambda^3}{6\eta}\left[F(x)-F(y)-(x-y)\frac{\mathrm{d}F(y)}{\mathrm{d}y}\right]-\frac{\lambda^3}{6}\left\{\frac{\partial x}{\partial\eta}\left[\frac{\mathrm{d}F(x)}{\mathrm{d}x}-\frac{\mathrm{d}F(y)}{\mathrm{d}y}\right]-\frac{\partial y}{\partial\eta}(x-y)\frac{\mathrm{d}^2F(y)}{\mathrm{d}y^2}\right\} \tag{9}$$

where $\beta=1/(kT)$, $x=\frac{(1+\lambda\psi)w}{\lambda^2}\beta\varepsilon$, $y=\frac{w\psi}{\lambda}\beta\varepsilon$ and the function $F(x)$ is given as:

$$F(x)=-\frac{1}{4}\ln(1-2x)-2\ln(1-x)-\frac{3}{2}x-\frac{1}{1-x}+1 \tag{10}$$

where w and ψ are expressed as:

$$w=6\eta/\phi_0^2 \tag{11}$$

$$\psi=\frac{\lambda^2(1-\eta)^2(1-e^{-\lambda})-12\eta(1-\eta)[1-\lambda/2-(1+\lambda/2)e^{-\lambda}]}{e^{-\lambda}L(\lambda)+S(\lambda)} \tag{12}$$

The variables α_0 and ϕ_0 in Eqs. (8) and (9) are defined as:

$$\alpha_0=\frac{L(\lambda)}{\lambda^2(1-\eta)^2} \tag{13}$$

$$\phi_0=\frac{\exp(-\lambda)L(\lambda)+S(\lambda)}{\lambda^3(1-\eta)^2} \tag{14}$$

The functions $L(\lambda)$ and $S(\lambda)$ are expressed as:

$$L(\lambda)=12\eta[(1+\eta/2)\lambda+1+2\eta] \tag{15}$$

$$S(\lambda)=(1-\eta)^2\lambda^3+6\eta(1-\eta)\lambda^2+18\eta^2\lambda-12\eta(1+2\eta) \tag{16}$$

The osmotic pressure and the chemical potential for the attractive contribution are expressed as:

$$\frac{\Pi^{\mathrm{yuk}}}{\varepsilon/\sigma^3}=T^*\rho^*Z^{\mathrm{yuk}} \tag{17}$$

$$\frac{\mu^{\mathrm{yuk}}}{kT}=\frac{A^{\mathrm{yuk}}}{NkT}+Z^{\mathrm{yuk}} \tag{18}$$

The reduced temperature T^* and reduced number density ρ^* are defined as:

$$T^*=kT/\varepsilon \tag{19}$$

$$\rho^*=\rho\sigma^3 \tag{20}$$

Liu *et al.*[13] used the above EOS with Yukawa potential and the λ value of 1.8 to describe the dispersion energy to 42 pure real fluids (including spherical, polar, chain-like and associated fluids). Liu's EOS was proved to be better than those with Lennard-Jones and Stockmayer potentials, and also better than the original SAFT EOS with Lennard-Jones or square well potentials as perturbation terms, respectively. So, in this paper the Yukawa potential with the λ value of 1.8 is used for all the real micelle, colloid and microemulsion systems.

Double-layer repulsion

The classical DLVO theory is widely used in the study of charged colloid and microemulsion systems from which the double-layer repulsion between two charged particles is represented by:[11]

$$u^{\mathrm{cc}}(r)=\frac{z^2e^2\exp[-\kappa(r-\sigma)]}{Dr(1+\kappa\sigma/2)^2}\quad(r>\sigma) \tag{21}$$

where ze is the charge on a particle, D is the dielectric constant of water, κ is the Debye screening parameter related to the number density of electrolytes:

$$\kappa^2=4\pi\sum_i\frac{\rho_i(z_ie)^2}{DkT} \tag{22}$$

z_i is the charge for a micro-ion i in solution.

The Helmholtz free energy for the double-layer repulsion can be expressed by Eq. (9) where $u^{\mathrm{att}}(|\mathbf{r}-\mathbf{r}'|)$ is replaced by the double-layer repulsion.

Because the double-layer repulsion has the same mathematic representation as the Yukawa potential, the Helmholtz free energy F^{cc} and the compressibility factor Z^{cc} have the same forms as Eqs. (8) and (9), except that the parameters ε and λ are replaced by ε' and λ', which are defined as:

$$\varepsilon'=-\frac{(ze)^2}{\sigma D(1+\kappa\sigma/2)^2} \tag{23}$$

$$\lambda'=\kappa\sigma \tag{24}$$

The double-layer repulsion between colloid and microemulsion particles can be rewritten in the form of:

$$u^{cc}(r)=\begin{cases}\infty & (r\leqslant\sigma)\\ \dfrac{-\varepsilon'\exp[-\lambda'(r/\sigma-1)]}{r/\sigma} & (r>\sigma)\end{cases} \tag{25}$$

The osmotic pressure and the chemical potential for the electrostatic contribution are expressed as:

$$\frac{\Pi^{cc}}{\varepsilon/\sigma^3}=T^*\rho^*Z^{cc} \tag{26}$$

$$\frac{\mu^{cc}}{kT}=\frac{A^{cc}}{NkT}+Z^{cc} \tag{27}$$

Results and discussion

Osmotic pressure

From Eqs. (4), (17) and (26), the osmotic pressure for dispersion systems can be expressed as:

$$\Pi=\Pi^{hs}+\Pi^{yuk}+\Pi^{cc} \tag{28}$$

Lin *et al.*[9] used the two-Yukawa EOS to describe the osmotic pressure for BSA-NaCl-H_2O charged colloid system. In this paper, we use one-Yukawa and two-Yukawa EOS to study the osmotic pressures for some uncharged micelle and microemulsion systems and weakly charged microemulsion systems, respectively.

Osmotic pressure for micelle systems

The *n*-alkyl polyoxyethylene ether molecule is abbreviated as C_xE_y, where C stands for the oleophilic alkyl group and E stands for the hydrophilic oxyethylene group, *x* and *y* are their group numbers in one molecule, respectively. The *n*-dodecyl hexaoxyethylene ether ($C_{12}H_{25}(C_2H_4O)_6H$, $C_{12}E_6$)-water micelle solution is a typical nonionic surfactant micelle system. Attwood *et al.*[14] reported plenty of the experimental osmotic pressure data for this system at different temperatures. The experimental osmotic pressure data in concentration range from 0.066 to 0.14 mol/L at 25, 27, 30 and 32.5 ℃ were given.

In our study, we treated the micelle as a hard sphere and supposed there are N_{agg} surfactant monomers aggregated in a micelle with a diameter of σ and K_{agg} ($K_{agg}=\frac{N_{agg}}{\sigma^3}$) is a constant. The relationship between the number density of surfactant monomers ρ_{mono} and the reduced number density of micelle ρ^* can be expressed as:

$$\rho_{mono}=\rho N_{agg}=\rho^*\frac{N_{agg}}{\sigma^3}=\rho^*K_{agg} \tag{29}$$

Because the aggregation number of surfactant in a micelle N_{agg} increases with the temperature,[14] it is reasonable to suppose the diameter of micelle is a monotone increasing function of the temperature. Li *et al.*[6] correlated it as:

$$\sigma=5.0857T-1433.70 \quad (10^{-10}\ \text{m}) \tag{30}$$

We use Eq. (30) in our study. Thus there are only two adjustable parameters in our EOS for uncharged micelles. They are K_{agg} and the dispersion energy ε. The water molecules are treated as the continuum. The experimental osmotic pressure data in concentration range from 0.066 to 0.1 mol/L at the four temperatures were fitted to obtain the adjustable parameters. The regressed parameters are: $K_{agg}=1.04\times10^{-3}$ ($10^{30}/m^3$), $\varepsilon/k=399.89$ K. The average relative deviation (ARD) of correlation for the osmotic pressures is 2.7%. The results are shown in Figure 1.

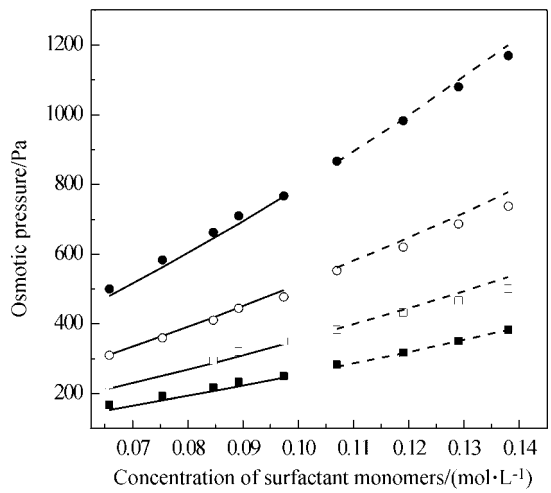

Figure 1 Correlated and predicted osmotic pressure values for $C_{12}E_6$-H_2O micelle system (symbols: experimental data, ●: 25.0 ℃, ○: 27.5 ℃, □: 30.0℃, ■: 32.5 ℃; — : correlated values, ----: predicted values).

By use of the regressed parameters, we predicted the osmotic pressure in concentration range from 0.1 to 0.14 mol/L at 25, 27, 30 and 32.5 ℃. The average relative deviation of prediction is 3.1%. The results are also shown in Figure 1. By using the hard sphere diameter σ and the correlated K_{agg}, we can also obtain the aggregation number N_{agg} of surfactant in a micelle. N_{agg} and σ of $C_{12}E_6$-water micelle at 25, 27, 30 and 32.5 ℃ are shown in Table 1.

Table 1 The aggregation number N_{agg} of surfactant and the hard sphere diameter σ of $C_{12}E_6$-H_2O micelle at 25, 27, 30 and 32.5 ℃

T/K	298.15	300.15	303.15	305.65
σ/nm	8.26	9.28	10.83	12.07
N_{agg}	586.13	830.41	1311.19	1830.76

Osmotic pressure for microemulsion systems

By treating the water molecules as the continuum and the microemulsion droplets as the hard sphere, the osmotic pressure in the uncharged and weakly charged microemulsion systems are studied.

The *n*-dodecyl pentaoxyethylene ether ($C_{12}E_5$)-decane ($C_{10}H_{22}$)-H_2O microemulsion system is uncharged. Bagger-Jörgensen *et al.*[3] successfully prepared the $C_{12}E_5$-$C_{10}H_{22}$-H_2O microemulsion system with spherical oil droplets, and measured the osmotic pressures of the system at 25.5 ℃. For such system, there are only two adjustable parameters ε and σ in the EOS. We correlated the experimental osmotic pressure data of the same system with the microemulsion droplet volume fraction range from 0.06 to 0.20 to get the adjustable parameters. The regressed ε/k is 93.45 K and σ is 128.42 $\times 10^{-10}$ m. The average relative deviation of correlation for osmotic pressures is 4.5%. The results are shown in Figure 2.

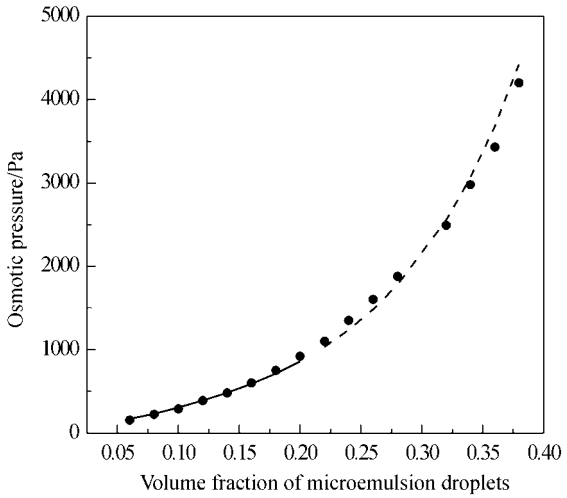

Figure 2 Correlated and predicted osmotic pressure values for $C_{12}E_5$-$C_{10}H_{22}$-H_2O microemulsion system at 25.5 ℃ (symbol: experimental data; — : correlated values, ----: predicted values).

By using the obtained parameters, we predicted the osmotic pressure data of this system with the microemulsion droplet volume fraction ranging from 0.20 to 0.38. The average relative deviation of prediction is 4.6%. The results are also shown in Figure 2.

Bagger-Jörgensen *et al.*[3] replaced small amount of the nonionic $C_{12}E_5$ by the anionic surfactant sodium dodecyl sulfate (SDS) and changed nonionic surfactant film into weakly charged one. In their research, osmotic pressures of $C_{12}E_5$-SDS-$C_{10}H_{22}$-H_2O microemulsion system at 25.5 ℃ were measured and reported.

For the above system, the electrovalence is very important for the osmotic pressure. Li *et al.*[6] proposed a method to determine the electrovalence and assumed that all of the ionic and nonionic surfactants are located in the micelle surfactant film. The total interface area of a microemulsion droplet equals to the sum of the sectional area occupied by the hydrophilic groups ($-C_2H_4O-$) in nonionic surfactant molecules and the hydrophilic groups ($-OSO_4^-$) in ionic surfactant molecules. The expression is as follows:

$$n_{SDS}\pi\left(\frac{\sigma_{-OSO_4^-}}{2}\right)^2+n_{C_{12}E_5}\pi\left(\frac{\sigma_{-C_2H_4O-}}{2}\right)^2=4\pi\left(\frac{\sigma}{2}\right)^2 \quad (31)$$

$$n_{SDS}=x\left(n_{SDS}+n_{C_{12}E_5}\right) \quad (32)$$

where x is the molar fraction of SDS in the surfactant mixture, n is the number of surfactant molecules in a droplet, $\sigma_{-OSO_4^-}$ is the diameter of the $-OSO_4^-$ in the ionic surfactant, $\sigma_{-C_2H_4O-}$ is the diameter of the $-C_2H_4O-$ in the nonionic surfactant, and σ is the diameter of the microemulsion droplet. Since the electrovalence of a droplet z is equal to the number of SDS in it, the electrovalence of a microemulsion droplet can be obtained from Eqs. (31) and (32) because of the electroneutrality in solution:

$$z=\frac{4x\sigma^2}{\sigma^2_{-C_2H_4O-}+x(\sigma^2_{-OSO_4^-}-\sigma^2_{-C_2H_4O-})} \quad (33)$$

Li *et al.*[6] correlated the diameters $\sigma_{-OSO_4^-}$ and $\sigma_{-C_2H_4O-}$ by using the cell model and they are 18.812 $\times 10^{-10}$ m and 9.413$\times 10^{-10}$ m, respectively. Their results were adopted directly here.

In this study, we assume the diameter σ of the microemulsion droplet is a function of the molar fraction x of SDS as follows:

$$\sigma=a+b/x \quad (10^{-10}\ \text{m}) \quad (34)$$

There are three adjustable parameters (a, b, ε) in our EOS. We correlated the osmotic pressure when x values are given as 0.01, 0.04 and 0.06 in the volume fraction range of 0.04 to 0.10 to obtain the adjustable parameters. The average relative deviation of correlation is 2.9%. The correlated parameters are: a=39.92, b=0.29, ε/k= 100.23 K. The correlated osmotic pressures agree well with the experimental data, which is shown in Figure 3. By use of the obtained parameters, we predicted the osmotic pressure in the volume fraction range of 0.10 to 0.25. The average relative deviation of prediction is 3.7%, which is also shown in Figure 3. We have also predicted the osmotic pressure in the case of x as 0.02, 0.03, 0.05 and 0.07. The results are shown in Figure 4.

From Figures 1—4, it can be seen that the calculated and the predicted osmotic pressures agree well with the experimental data. We have compared our results with those of Li *et al.*[6] The comparison shows that our results are a bit better than those from Li *et al.*, which proves the EOS proposed in this work is appropriate. The comparison is shown in Table 2.

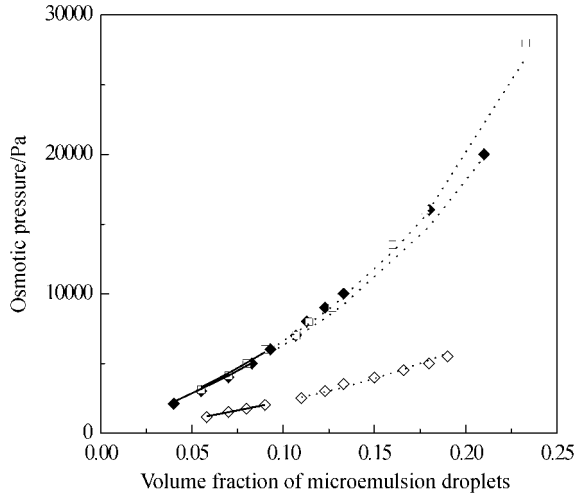

Figure 3 Correlated osmotic pressure values for $C_{12}E_5$-$C_{10}H_{22}$-SDS-H_2O microemulsion system at 25.5 ℃ (symbols: experimental data, ◇: x=0.01, ◆: x=0.04, □: x=0.06; —: correlated values, ----: predicted values).

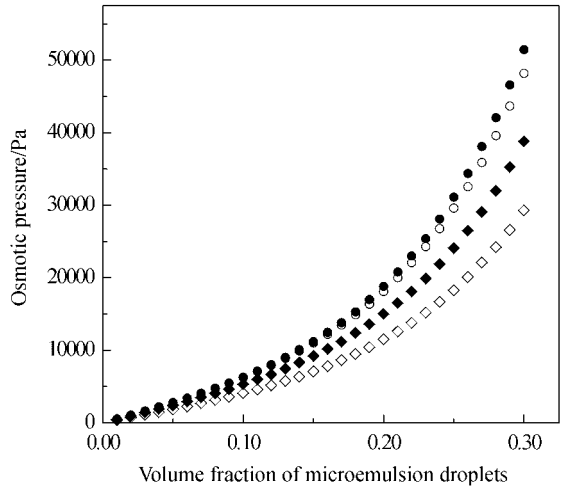

Figure 4 Predicted osmotic pressure values for $C_{12}E_5$-$C_{10}H_{22}$-SDS-H_2O microemulsion system at 25.5 ℃ (symbols: predicted data, ◇: x=0.02, ◆: x=0.03, ○: x=0.05; ●: x=0.07) .

Liquid-liquid equilibrium

For dispersion systems, the osmotic pressure and the chemical potential can be expressed as:

$$\Pi=\Pi^{hs}+\Pi^{yuk}+\Pi^{cc}$$

$$\mu=\mu^{hs}+\mu^{yuk}+\mu^{cc} \tag{35}$$

The liquid-liquid equilibrium between upper and lower phases requires osmotic pressure and chemical potential in both phases to be equal:

$$\begin{cases}\Pi^{I}=\Pi^{II}\\ \mu^{I}=\mu^{II}\end{cases} \tag{36}$$

Table 2 Comparison between Li's[6] results and this work

	Systems	Li *et al.*	This work
Used model	uncharged systems	cell model	Yukawa potential
	charged systems	cell model +MSA	Two-Yukawa potential
ARD of correlation/%	$C_{12}E_6$-H_2O	3.5	2.6
	$C_{12}E_5$-$C_{10}H_{22}$-H_2O	5.2	4.4
	$C_{12}E_5$-$C_{10}H_{22}$-H_2O-SDS	5.1	2.9
ARD of prediction/%	$C_{12}E_6$-H_2O	2.0	2.7
	$C_{12}E_5$-$C_{10}H_{22}$-H_2O	2.8	4.6
	$C_{12}E_5$-$C_{10}H_{22}$-H_2O-SDS	4.5	3.7
Adjustable parameters	$C_{12}E_6$-H_2O	2	2
	$C_{12}E_5$-$C_{10}H_{22}$-H_2O	2	3
	$C_{12}E_5$-$C_{10}H_{22}$-H_2O-SDS	4	3

By use of our EOS, we firstly studied the osmotic pressure and the liquid-liquid phase equilibrium for Yukawa fluids. By solving Eq. (36), the reduced number densities and the reduced osmotic pressure were obtained simultaneously. The reduced osmotic pressures Π^* are shown in Figure 5, the reduced number densities ρ^* are shown in Figure 6. From Figure 6, it can be seen that the upper critical solution temperature T_c descends with the increase of the range parameter λ. The T_c values thus obtained are 1.52, 1.24 and 1.05 when the λ values are 1.5, 1.8 and 2.1, respectively.

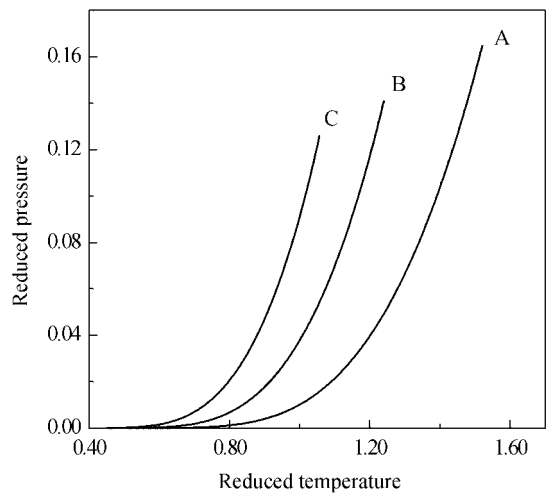

Figure 5 Reduced osmotic pressure for micelle and microemulsion systems at phase equilibrium (A: λ=1.5, B: λ=1.8, C: λ=2.1).

We also applied our EOS to some real uncharged micelle and charged colloid systems.

Liquid-liquid equilibrium for uncharged micelle systems

The phase diagrams for C_xE_y-H_2O systems are characterized by a closed loop with a region of immiscibility between two dense fluids, bounded by upper critical

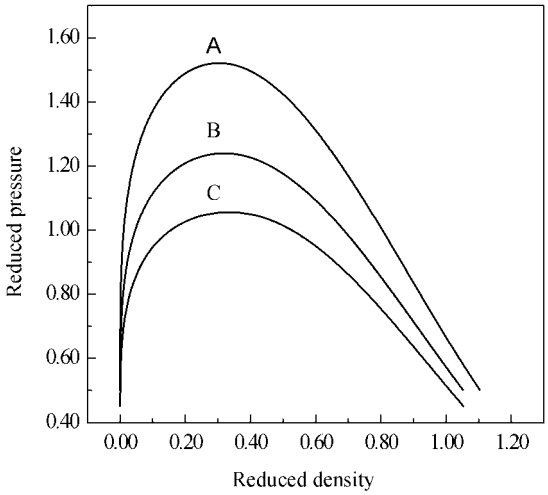

Figure 6 Reduced density for micelle and microemulsion systems at phase equilibrium (A: λ=1.5, B: λ=1.8, C: λ=2.1).

solution temperature (UCST) and lower critical solution temperature (LCST). The two liquids separate spontaneously into immiscible phases between the UCST and LCST. However, they are completely miscible above the UCST and below the LCST. Lang *et al.*[15] presented a phase diagram for mixtures of 3,6,9,12-tetraoxadocosanol ($C_{10}E_4$) with water. Aizpiri *et al.*[16] measured the closed-loop coexistence curve for 2-butoxyethanol-water system with special attention to the region near the LCST. Lim *et al.*[17] determined the coexistence curves for binary mixtures of 2-(2-hexyloxyethoxy) ethanol (C_6E_2) with water around the LCST. Rudolph *et al.*[18] reported the experimental liquid-liquid phase equilibrium data of the systems *n*-hexyltetraoxyethylene (C_6E_4)-water and *n*-heptyltetraoxyethylene (C_7E_4)-water at pressures up to 100 MPa and in the temperature range between 315 and 355 K. Andersen *et al.*[19] investigated the influence of pressure and temperature on the phase behavior of the systems C_4E_1-water-octane and C_4E_2-water-octane.

In recent years, many thermodynamic researches have been made in this field. Knudsen *et al.*[20] studied binary *n*-butoxyethanol-water (C_4E_1-H_2O) and 2-butanol-water systems by UNIQUAC G^E model combined with the SRK-EOS. Garcia-Lisbona *et al.*[21] predicted the high pressure phase equilibria for binary aqueous solutions of 1-butanol, C_4E_1 and *n*-decylpentaoxyethylene ether ($C_{10}E_5$) with the SAFT-HS EOS. Rudolph *et al.*[18] studied the phase behavior of water-C_xE_y (including C_4E_1, C_6E_3, C_6E_4, C_7E_3, C_7E_4 and C_7E_5) systems by Peng-Robinson equation of state with the Wong-Sandler mixing rules and the UNIQUAC G^E-model. Andersen *et al.*[19] studied the phase behavior of systems C_4E_1-water-octane and C_4E_2-water-octane with the SAFT HS EOS.

In this paper, all the concentrations of surfactant C_xE_y in both phases for C_xE_y-H_2O systems are larger than their CMC. For example, the CMC of $C_{10}E_4$ at 25 ℃ is nearly 7.0×10^{-4} mol/L,[22] while from the phase equilibrium diagram of $C_{10}E_4$-H_2O system, it can be seen that the minimum and the maximum molar concentrations of $C_{10}E_4$ are nearly 2.4×10^{-3} mol/L and 2.5 mol/L, respectively. Hence all the solutes in the mentioned systems can be considered as micelles and the water is treated as the continuum. We use this primitive model to study the liquid-liquid equilibria for C_4E_1-H_2O, C_6E_2-H_2O and $C_{10}E_4$-H_2O systems.

The reduced number densities of micelles ρ^* ($\rho^*=\rho\sigma^3$) in upper phase and lower phase can be obtained by minimizing Eq. (36). When the ρ^* are obtained, the number densities of the surfactant monomers in upper and lower phases can be expressed as:

$$\rho^{\mathrm{I}}_{\mathrm{mono,cal}}=\rho^{*\mathrm{I}}\frac{N_{\mathrm{agg}}}{\sigma^3}=\rho^{*\mathrm{I}}K_{\mathrm{agg}}$$

$$\rho^{\mathrm{II}}_{\mathrm{mono,cal}}=\rho^{*\mathrm{II}}\frac{N_{\mathrm{agg}}}{\sigma^3}=\rho^{*\mathrm{II}}K_{\mathrm{agg}} \tag{37}$$

where the subscript mono stands for the monomer of surfactant molecule.

The cross dispersion energy ε/k is expressed as a function of temperature. The adjustable parameters for one micelle are regressed by minimizing the objective function:

$$f=(\rho^{\mathrm{I}}_{\mathrm{mono,cal}}/\rho^{\mathrm{I}}_{\mathrm{mono,exp}}-1.0)^2+(\rho^{\mathrm{II}}_{\mathrm{mono,cal}}/\rho^{\mathrm{II}}_{\mathrm{mono,exp}}-1.0)^2 \tag{38}$$

By minimizing Eqs. (36) and (38), the number densities of the surfactant monomers in both phases and the adjustable parameters were obtained simultaneously. The phase diagrams are shown in Figures 7—9. The

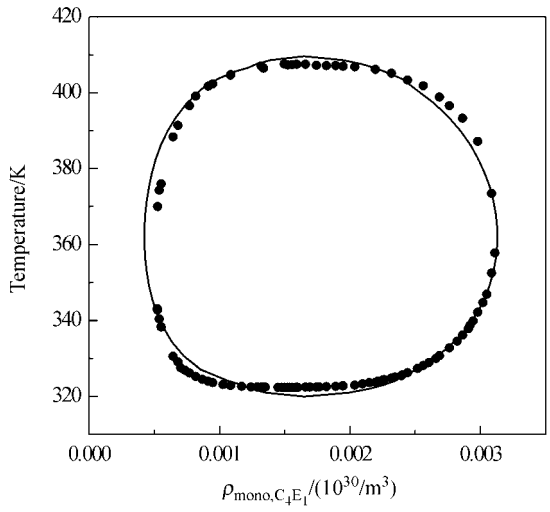

Figure 7 Liquid-liquid phase equilibria for C_4E_1-H_2O system (symbols: experimental data, line: correlated values).

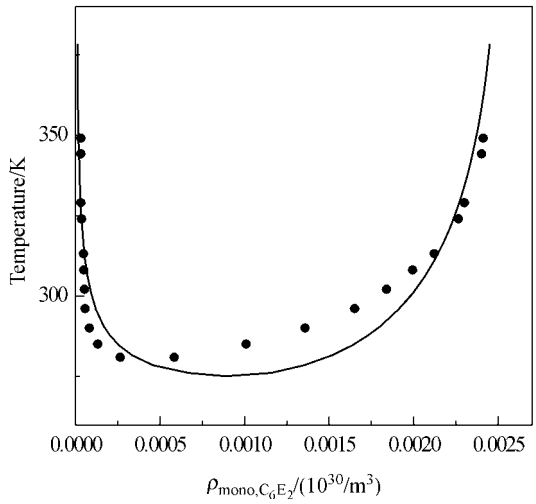

Figure 8 Liquid-liquid phase equilibria for C_6E_2-H_2O system (symbols: experimental data, line: correlated values).

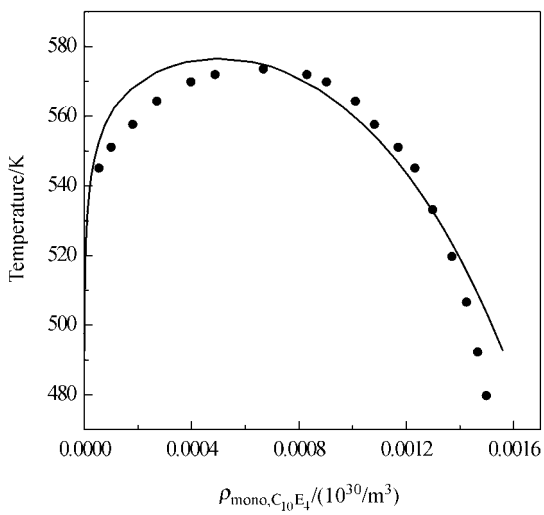

Figure 9 Liquid-liquid phase equilibria for $C_{10}E_4$-H_2O system (symbols: experimental data, line: correlated values).

parameters ε/k and K_{agg} are shown in Table 3. The ε/k values at 373.15 K are also listed in Table 3. We find when the molecular weights of the surfactants increase, the ε/k values increase while the K_{agg} values decrease.

Table 3 Correlated ε/k and K_{agg} for C_4E_1-H_2O, C_6E_2-H_2O and $C_{10}E_4$-H_2O micelle systems

Systems	ε/k (K)	ε/k (K) at 373.15 K	K_{agg} ($10^{30}/m^3$)
C_4E_1-H_2O	$-2767.31+16.22T-0.021T^2$	361.1236	5.10×10^{-3}
C_6E_2-H_2O	$1275.53-2.82\times10^5/T$	519.8017	2.79×10^{-3}
$C_{10}E_4$-H_2O	$-2075.13+1.47\times10^6/T$	1864.305	1.56×10^{-3}

We can make a brief comparison among the UNIQUAC G^E-model, the SAFT-HS EOS and ours. From literatures 18—21, we can see the UNIQUAC G^E-model and the SAFT-HS EOS can describe the phase equilibria for C_xE_y-H_2O systems satisfactorily. However, there are large numbers of adjustable parameters in both the UNIQUAC G^E-model and the SAFT-HS EOS. In our EOS, there are only three or four parameters for such complicated systems and the results also agree well with the experimental data. It seems the primitive model is of a good approach for the liquid-liquid equilibria for micelle solutions. On the other hand, the UNIQUAC G^E-model and the SAFT-HS EOS can be used to describe the influence of pressure on the phase behavior for C_xE_y-H_2O systems, and it is difficult to apply our EOS to LLE for C_xE_y-H_2O systems at high pressure.

Liquid-liquid equilibria and the osmotic pressure for charged colloid systems

Victor *et al.*[23] reported the existence of temperature-induced liquid-liquid separation of lysozyme-sodium phosphate-water solutions with the pH values of 6.0, 6.5 and 7.0 and the ionic strength value of 0.6 mol/L. We studied the phase equilibria of such systems by using the primitive model.

In our work, the colloid particle is considered as a hard sphere surrounded by an electric double layer, the water molecules are treated as the continuum. The hard sphere repulsion between colloid particles is expressed by the Carnahan-Starling equation. The dispersion interaction and the double layer repulsion between colloid particles are expressed by two Yukawa potentials. The Donnan effect on phase equilibrium is ignored because it is very small. During the calculation, four parameters are needed: the net charge z on each colloid particle, the molecular weight M, the hard sphere diameter σ and the dispersion energy ε/k. The net charge z is dependent on the pH value. From Kuehner *et al.*'s work,[24] we got the lysozyme net charges z as 8.5, 8.0 and 7.5 at pH values of 6.0, 6.5 and 7.0, respectively. The hard sphere diameter σ is adopted as 3.44 nm from Victor *et al.*[23]. The experimental data at pH values of 6.0, 6.5 and 7.0 are used to correlate the dispersion energy ε/k and molecular weight M. The objective function used in the correlation is defined as:

$$f=(\rho^{I}_{cal}/\rho^{I}_{exp}-1.0)^2+(\rho^{II}_{cal}/\rho^{II}_{exp}-1.0)^2 \quad (39)$$

By minimizing Eqs. (36) and (39), the number density of lysozyme molecules in both phases and the adjustable parameters ε/k and M were obtained simultaneously. We assume the dispersion energy ε/k is a function of temperature. The dispersion energy is regressed as follows:

$$\varepsilon/k=-1001.4+3.3\times10^5/T \ \ (K) \quad (40)$$

the molecular weight M is regressed as 17700 g/mol. The liquid-liquid equilibrium diagrams are shown in Figure 10. This figure shows that although there are

only two adjustable parameters and the studied systems are very complicated, the coexistence curves calculated by our EOS agree well with the experimental data. The results indicate that our EOS has good ability to describe the phase equilibria for colloid systems in a wide temperature range.

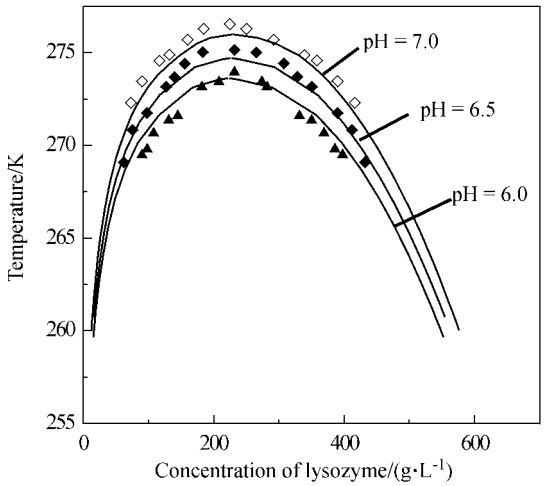

Figure 10 Liquid-liquid phase equilibria for lysozyme-Na_3PO_4-H_2O systems correlated by two-Yukawa potentials (symbols: experimental data, line: correlated values).

In order to test the prediction function of our EOS, we predicted the osmotic pressure for lysozyme-ammonium sulfate-water, lysozyme-ammonium oxalate-water and lysozyme-ammonium phosphate-water systems at 25 ℃[7] by using the parameters σ, ε/k and M mentioned above.

Commonly, the Donnan effect is often taken into account when we consider the osmotic pressure for protein systems. The osmotic pressure is presented in the following form:

$$\Pi=\Pi^{hs}+\Pi^{yuk}+\Pi^{cc}+\Pi^{donnan} \tag{41}$$

where $\Pi^{donnan}=Z^{donnan}\rho_p kT$ is the osmotic pressure due to the Donnan effect. The compressibility factor Z^{donnan} is expressed as:

$$Z^{donnan}=(\rho_+^{in}+\rho_-^{in}-\rho_+^{out}-\rho_-^{out}) \tag{42}$$

where ρ_p, ρ_+, ρ_- and z_p, z_+, z_- are the number densities and the charge numbers of proteins, micro-cation and micro-anion, respectively. The superscripts in and out stands for the protein side and micro-ion side, respectively. ρ_p, ρ_+, ρ_- can be obtained by solving the following equations:

$$z_+\rho_+^{out}+z_-\rho_-^{out}=0 \tag{43}$$

$$z_p\rho_p+z_+\rho_+^{in}+z_-\rho_-^{in}=0 \tag{44}$$

$$(\rho_+^{in})^{|z_-|}(\rho_-^{in})^{|z_+|}=(\rho_+^{out})^{|z_-|}(\rho_-^{out})^{|z_+|} \tag{45}$$

The osmotic pressures for lysozyme-ammonium sulfate-water, lysozyme-ammonium oxalate-water and lysozyme-ammonium phosphate-water systems (117 experimental data in total) at 25 ℃ are predicted. The average relative deviation of prediction is 3.85% when the Donnan effect is taken into account and 3.99% when it is ignored. The results are shown in Figures 11—15. It seems the two-Yukawa potential is suitable for charged colloid systems and the EOS in this study has not only the correlation function but also the prediction function for such systems.

The results are shown in Figures 11—15. It seems that the two-Yukawa potential is suitable for charged colloid systems and the EOS in this study has not only the correlation function but also the prediction function for such systems.

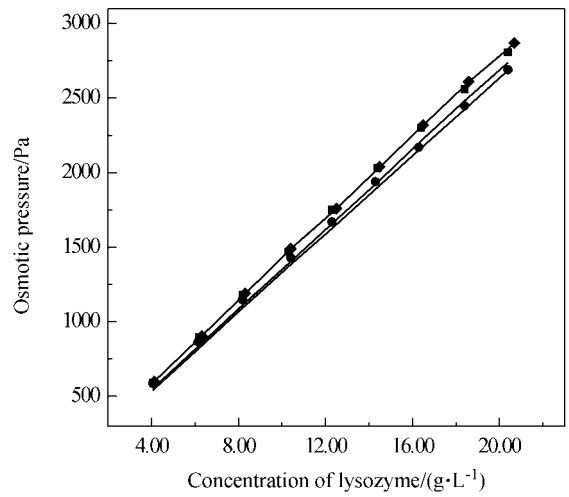

Figure 11 Predicted osmotic pressure values for lysozyme-$(NH_4)_2SO_4$-H_2O systems at 25 ℃, ionic strength=1.0 mol/L (symbols: experimental data, ◆: pH=4.0, ■: pH=7.0, ●: pH=8.0, line: predicted values).

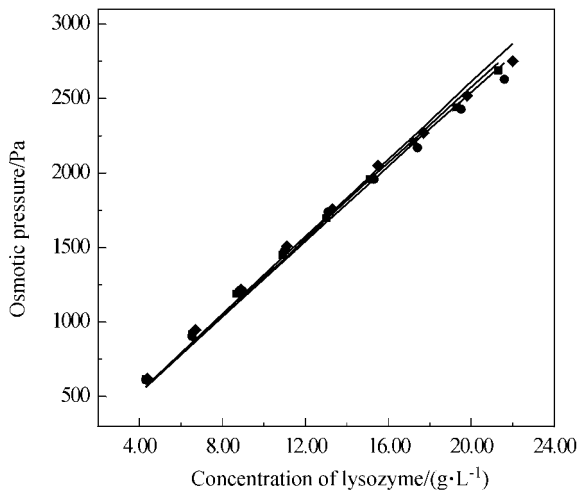

Figure 12 Predicted osmotic pressure values for lysozyme-$(NH_4)_2SO_4$-H_2O systems at 25 ℃, ionic strength=3.0 mol/L (symbols: experimental data, ◆: pH=4.0, ■: pH=7.0, ●: pH=8.0, line: predicted values).

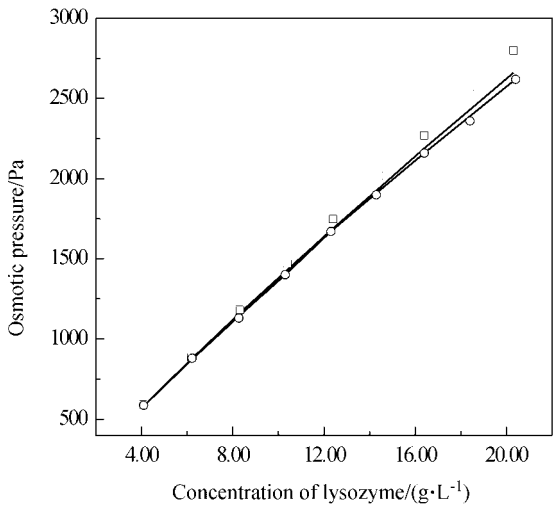

Figure 13 Predicted osmotic pressure values for lysozyme-$(NH_4)_2HPO_4$-H_2O systems at 25 ℃, pH=7.0 (symbols: experimental data. □: ionic strength=1.0 mol/L, ○: ionic strenhth=3.0 mol/L, line: predicted values).

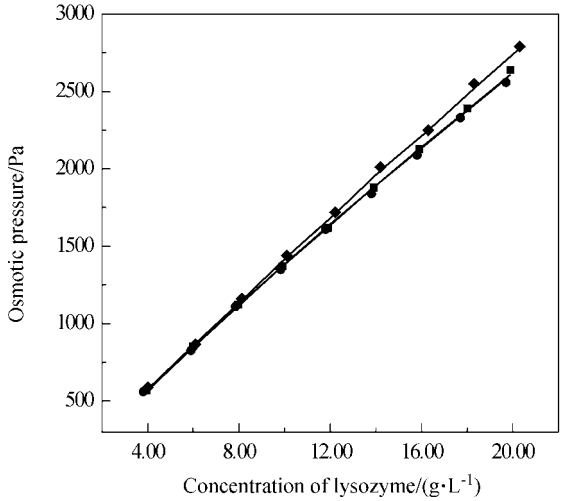

Figure 14 Predicted osmotic pressure values for lysozyme-$(NH_4)_2C_2O_4$-H_2O systems at 25 ℃, ionic strength=1.0 mol/L (symbols: experimental data, ◆: pH=4.0, ■: pH=7.0, ●: pH=8.0, line: predicted values).

Discussion

The range parameter λ in Yukawa potential plays an important role in the osmotic pressure and the phase diagram, which has been studied in this work. The thermodynamic and structural properties with Yukawa potential are qualitatively similar to those with LJ potential when the range parameter λ is taken as 1.8, which was pointed out by Henderson *et al.*[25] So in this study we choose the λ value as 1.8 for all the real systems.

For the micelle systems, the relationship between the number density of surfactant monomers ρ_{mono} and the reduced number density of micelle ρ^* is necessary both in the study on osmotic pressure and the phase equilibrium. We obtained the relationship by using a

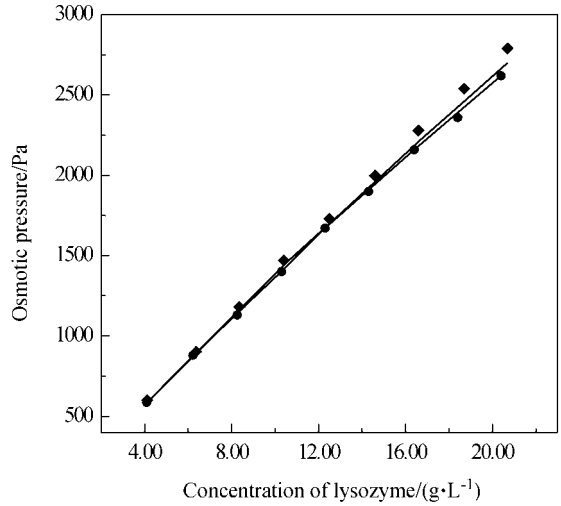

Figure 15 Predicted osmotic pressure values for lysozyme-$(NH_4)_2HPO_4$-H_2O systems at 25 ℃, pH=8.0 (symbols: experimental data. ◆: ionic strenhth=1.0 mol/L, ●: ionic strength=3.0 mol/L, line: predicted values).

constant K_{agg} to express the ratio of $\frac{N_{agg}}{\sigma^3}$. The correlated K_{agg} values for C_4E_1-H_2O, C_6E_2-H_2O, $C_{10}E_4$-H_2O and $C_{12}E_6$-H_2O systems seem reasonable, and they decrease with the increase of molecular weight of the surfactants. The aggregation number N_{agg} for $C_{12}E_6$-H_2O system increases with temperature, which is also reasonable. It seems that the parameters in our EOS have physical meanings.

In our study, we only use one dispersion energy parameter ε instead of the three parameters ε_{11}, ε_{22} and ε_{12} in DLVO theory in order to simplify our calculation. The ε/k values for C_4E_1-H_2O, C_6E_2-H_2O and $C_{10}E_4$-H_2O at 373.15 K (which are listed in Table 3) show that the tendency that they increase with molecular weight of surfactants is reasonable.

In the investigated micelle and microemulsion systems, the dispersed particles deform when they are close to each other. The deformation mainly influences the volume fraction of particles. Though the deformation is not important in the study of osmotic pressure, it plays a very important role in the phase equilibria. However, as the Yukawa EOS is on the basic of hard-core Yukawa potential, it is difficult to take the deformation into account in this paper. We only investigated the phase equilibria for micelle solutions because deformation of micelle particle is very small and there is an additional adjustable parameter K_{agg}, which makes the calculated results satisfactory compared with the experimental data.

Conclusion

A new equation of state for dispersion systems has been established. The hard sphere repulsion is expressed by the Carnahan-Starling equation. The Hamaker potential in DLVO theory is replaced by the Yukawa potential

to describe the attractive interaction. Because the double-layer repulsion is in the same form as the Yukawa potential, the electrostatic contribution to the osmotic pressure and the chemical potential has the same representation as the dispersion contribution. Our EOS is simple because there are only two or three contribution terms and a few adjustable parameters for such complicated dispersion systems.

By treating the water molecules in such systems as the continuum, the primitive model combined with the established EOS is used to study the liquid-liquid equilibria. The adjustable parameters have some physical meanings.

Both the results of osmotic pressure and liquid-liquid equilibria agree well with the experimental data, which proves that the primitive model is of an appropriate method for micelle, colloid and microemulsion systems and that the EOS developed in this paper has a good capability both in correlation and prediction.

References

1 Kaler, E. W.; Bennett, K. E.; Davies, H. T. *J. Chem. Phys.* **1983**, *79*, 5673.

2 Hill, T. L. *An Introduction to Statistical Thermodynamics*, Addison & Wesley, Reading, Massachusetts, **1960.**

3 Bagger-Jörgensen, H.; Olsson, U.; Jönsson, B. *J. Phys. Chem. B* **1997**, *101*, 6504.

4 Denkov, N. D.; Petsev, D. N.; Danov, K. D. *Phys. Rev. Lett.* **1993**, *71*, 3226.

5 Petsev, D. N.; Linse, P. *Phys. Rev. E* **1997**, *55*, 586.

6 Li, X.-S.; Lu, J.-F.; Li, Y.-G. *Ind. Eng. Chem. Res.* **1999**, *38*, 2812.

7 Moon, Y. U.; Anderson, C. O.; Blanch, H. W. *Fluid Phase Equilibria* **2000**, *168*, 229.

8 Wu, J.-Z.; Prausnitz, J. M. *Fluid Phase Equilibria* **1999**, *155*, 139.

9 Lin, Y. Z.; Li, Y. G.; Lu, J. F. *Acta Chim. Sinica* **2001**, *59*, 2110 (in Chinese).

10 Carnahan, N. F.; Starling, K. E. *J. Chem. Phys.* **1969**, *51*, 635.

11 Verwey, E. J. W.; Overbeek, J. T. C. *Theory of the Stability of Lyophobic Colloids*, Elsevier Publishing Company, New York, **1948.**

12 Duh, D.M., Mier-Y-Teran, L. *Mol. Phys*. **1997**, *90, 373.*

13 Liu, Z.-P.; Li, Y.-G.; Chan, K.-Y. *Ind. Eng. Chem. Res.* **2001**, *40*, 973.

14 Attwood, D.; Elworthy, P. H.; Kayne, S. B. *J. Phys. Chem.*, **1970**, *74*, 3529.

15 Lang, J. C.; Morgan, R. D. *J. Chem. Phys*., **1980**, *73*, 5849.

16 Aizpiri, A.G.; Monroy, F.; del Campo, C. *J. Chem. Phys.* **1992**, *165*, 31.

17 Lim, K. H.; Reckley, J. S.; Smith, D. H. *J. Colloid Interface Sci*. **1993**, *161*, 465.

18 Rudolph, E. S. J.; Langeveld, J. H.; de Loos, T. W. *Fluid Phase Equilibria* **2000**, *173*, 81.

19 Andersen, J. G.; Koak, N.; de Loos, T. W. *Fluid Phase Equilibria* **1999**, *163*, 259.

20 Knudsen, K.; Stenby, E. H.; Anderson, J. G. *Fluid Phase Equilibria* **1994**, *93*, 55.

21 Garcia-Lisbona, M. N.; Galindo, A.; Jackson, G. *Mol. Phys.* **1998**, *93*, 57.

22 Li, X.-S.; Lu J.-F.; Li, Y.-G. *Fluid Phase Equilibria* **1998**, *153*, 215.

23 Victor, G. T.; Andreas, H.; George, M. T. *J. Phys. Chem.* **1990**, *94*, 2140.

24 Kuehner, D. E.; Engmann, J.; Fergg, F. *J. Phys. Chem. B* **1999**, *103*, 1368.

25 Henderson, D.; Waisman, E., Lebowitz, J. L. *Mol. Phys.* **1978**, *35*, 241.

(E0311133 ZHAO, X. J.)